Annals of Arid Zone 64(4): 537-554, 2025

Impact of Time Resolution of Rainfall Measurement on Erosivity Factor in Arid Region of India

Deepesh Machiwal*, Priyabrata Santra, H.M. Meena and Akath Singh[1]

Division of Natural Resources, ICAR-Central Arid Zone Research Institute, Jodhpur 342 003, India

[1]Current Address: Division of Post Harvest Management, Central Institute of Subtropical Horticulture, Lucknow 226 101, India

Received: June 26, 2025 Accepted: August 1, 2025

Abstract: Rainfall erosivity is considered as a vital factor in computing soil loss through erosion prediction models such as original and derived versions of the universal soil loss equation model. The accurate estimates of the rainfall erosivity require high-resolution rainfall measurements, which are still not widely available for many parts of the world. In this study, a set of conversion factors was developed to adjust rainfall erosivity estimates derived from rainfall data recorded at various temporal resolutions to those based on 1 min interval rainfall measurements. For the first time in the western arid region of India, 1 min interval rainfall data for two years (2020 and 2024) were utilized to compute the total kinetic energy (E), maximum 30 minute rainfall intensity (I_{30}), and rainfall erosivity factor (R-factor) for individual rainfall events using the EI_{30} index method. Results of the study indicated that I_{30} values were severe for 5% to 10% of the total rainy storms, and high to very high for 75% to 80% storms. It is further revealed that as rainfall measurement interval decreases, the peaks of I_{30} are easily captured, which ultimately leads to enhanced erosive energy of the rainfall. The conversion factors obtained for the arid region in this study are relatively less as compared to that reported for humid and semi-arid regions in earlier studies. Also, underestimations of the E are evidenced on increasing the time interval from 5 min to 60 min with relative error within -10% whereas, the R-factors showed -4.5, -8.0, -9.6, -5.8 and -96.7% underestimations at 5, 15, 30 and 60 min and 24 h, respectively. The relationships developed for computing the precise and accurate E, I_{30} and R-factors for high-resolution (1 min) data based on coarser data at different time intervals (5 min, 15 min, 30 min, 60 min and 24-h) can be used adequately as the estimations involves a strong interactions confirmed among the factors.

Key words: High temporal resolution; kinetic energy; maximum 30 min rainfall intensity; arid region; conversion factor.

Land degradation, defined as the replacement of climax vegetation with deprived vegetation, adversely impacts soil

OPEN ACCESS

Editor-in-Chief
Praveen Kumar

Editors (India)
Anita Pandey
Hema Yadav
Neena Singla
Ritu Mawar
Sanjana Reddy
Surendra Poonia
R.K. Solanki
P.S. Khapte

Editors (International)
M. Faci, Algeria
M. Janmohammadi, Iran

Correspondence
Deepesh Machiwal
dmachiwal@rediffmail.com

Citation
Machiwal, D., Santra, P. Meena, H.M. and Singh, A. 2025. Impact of time resolution of rainfall measurement on erosivity factor in arid region of India. Annals of Arid Zone 64(4): 537-554

https://doi.org/10.56093/aaz.v64i4.168282

https://epubs.icar.org.in/index.php/AAZ/article/view/168282

quality and ecosystem services (Lal, 2012). Thus, it is a threat to sustainable development globally and presents a great challenge in arid regions of the world that encompasses about 41% of the terrestrial area (Zhang *et al*., 2015). In India, land and soil degradation are pervasive problems that pose a serious threat to the country's food and nutrition security (Bhattacharyya *et al*., 2015). According, to the harmonized database of the Government of India, about 120.7 m ha land of the country is degraded (NAAS, 2012). Furthermore, the country loses about 5.3 billion tons of soil annually (Katsir *et al*., 2024). Hence, soil erosion due to water (83.31 m ha) and wind (11.56 m ha) is the primary cause of soil degradation in the country, followed by soil acidity (17.93 m ha), sodic soils (3.71 m ha), soil salinity (2.73 million ha), water logging (0.91 million ha), and mining and industrial waste (0.26 m ha) (ICAR and NAAS, 2010). It has been further reported that soil erosion diminishes crop yields and inclines agricultural water use, which ultimately leads to $8 billion economic loss globally as well as $1500 million annual loss in India (Sartori *et al*., 2019).

In India, the western arid region—primarily encompassing parts of Rajasthan and Gujarat—has historically experienced severe wind erosion, which has been identified as a major contributor to land degradation since ancient times (Santra *et al*., 2014). Conversely, water-induced soil erosion has generally not been regarded as a serious concern in this region, owing to the relatively infrequent, low-intensity, and low-volume rainfall events that were traditionally considered to have minimal impact on soil loss (Machiwal *et al*., 2016). However, since the beginning of the 21st century, increase in rainfall depth and intensity are being observed in different parts of the world caused by climate change (IPCC, 2007). The rise in global air temperature and increase in rainfall amount and intensity along with their inclining trends are further confirmed by the general circulation models (IPCC, 2001; IPCC, 2012). Globally, rainfall extremes have been recorded with increasing frequency, with the most pronounced increases observed in tropical regions. For instance, a recent study reported that one in every four record-breaking rainfall events occurred during the decade 2011–2020 (Robinson *et al*., 2021). Likewise, the Indian arid regions are also witnessing rising rainfall trends, recently reported in the literature (e.g., Machiwal *et al*., 2017; Meena *et al*., 2019). In certain parts of the Indian arid region, rainfall intensity is extremely high, with approximately 38% to 68% of the annual rainfall occurring within just 48 to 96 hours (Machiwal *et al*., 2015). The rainfall patterns over the last one decade clearly revealed that soil erosion due to water cannot simply be neglected in the arid region of India.

In literature, several methods have been evolved or developed for estimating soil erosion depending upon the data availability and factors causing erosion (Machiwal *et al*., 2022). Rainfall erosivity (R) factor is adjudged as the best indicator to measure potential ability of a rainstorm to cause soil erosion as it combines the raindrop impact on the soil detachment and the turbulence of runoff to transport the dislodged soil particles (Porto, 2016). The R-factor plays an important role in the soil erosion prediction models such as universal soil loss equation (USLE) (Wischmeier and Smith, 1978), modified universal soil loss equation (MUSLE) (Williams and Berndt, 1972) and revised universal soil loss equation (RUSLE) (Renard, 1997). Computation of the R-factor is of paramount significance and is mostly done by using EI_{30} index method as defined in the USLE model. The EI_{30} method correlates the soil eroded from the single rainfall event with the product of kinetic energy (E) of the storm and 30 min maximum rainfall intensity (I_{30}) (Wischmeier and Smith, 1978). There have been different statistical models of the EI_{30} method depending upon the temporal scale of the rainfall data such as daily (Xie *et al*., 2016), monthly (Yu and Rosewell, 1996) and annual rainfall (Renard and Freimund, 1994). Many researchers evaluated the accuracy of the soil erosion prediction models using different resolution rainfall data and reported that the prediction accuracy improves on enhancing the temporal resolution (e.g., Yin *et al*., 2015). Traditionally, rainfall recorded through non-recording rain gauges yielded data at daily (24 h) interval, which were found adequate for the computation of R-factor. However, with technological advancement, rainfall monitoring through tipping bucket mechanism and automatic digital recording allowed reduction in the rainfall monitoring interval up to less

than 24 h. Accordingly, the R-factor has been estimated using fixed-interval data of 5 min (Diodato *et al*., 2017; Fiener *et al*., 2013; Martins *et al*., 2010), 6 min (Mcfarlane *et al*., 1986; Yu, 1998), 10 min (Hanel *et al*., 2016; Klik *et al*., 2015; Meusburger *et al*., 2012; Santosa *et al*., 2010; Schmidt *et al*., 2016; Verstraeten *et al*., 2006) and 15 min or 30 min (Mannaerts and Gabriels, 2000; Panagos *et al*., 2016; Shamshad *et al*., 2008). Thus, accurate estimation of the R-factor is important to enhance prediction performance of the soil erosion models.

This study is undertaken with an objective to estimate R-factor, for the first time, in the western arid region of India based on high-resolution rainfall monitored at 1 min interval. Furthermore, conversion factors are computed to convert R-factor estimated from coarser resolution data to that predicted from the high-resolution data. The study estimated R factors using rainfall data recorded at 1 min interval and then aggregated to 5 min, 10 min, 15 min, 30 min, 60 min and 24 h. It is revealed from the literature that such studies conducted for any region of India are rarely available.

Materials and Methods

***Study Area and Data Description*:** One digital rainfall recorder (Virtual Hydromet, India) with a resolution of 0.2 mm was established at a height of 1.5 m in research farm of the Central Arid Zone Research Institute (CAZRI), Jodhpur, India in the year 2020. In this study, rainfall data were recorded by digital rainfall recorder at 1 min time interval during monsoon season (July through September) for two years, i.e., 2020 and 2024. The recorded data were downloaded from the recorder at weekly interval and were imported to Microsoft Excel for further analyses. The data quality was verified by comparing daily rainfall totals calculated from 1 min data with those measured from the ordinary rain gauge installed at agro-meteorological observatory of CAZRI, Jodhpur. The scattered plot drawn between calculated and measured daily rainfall totals showed a close resemblance with 1:1 line (Fig. 1). Values of correlation coefficient (r = 0.98), coefficient of determination (R^2 = 0.96) and standard error (0.24 mm) between 24 h recorded and measured rainfall totals further confirmed accuracy of the recorded data. Rainfall records at 1 min time interval were not available for the past in this arid region as it was not considered important in historical times looking at low magnitude and rare occurrence of the extreme rainfall events. The recorded 1 min rainfall data of the two years were accumulated to 5, 15, 30 and 60 min and 24 h rainfall data.

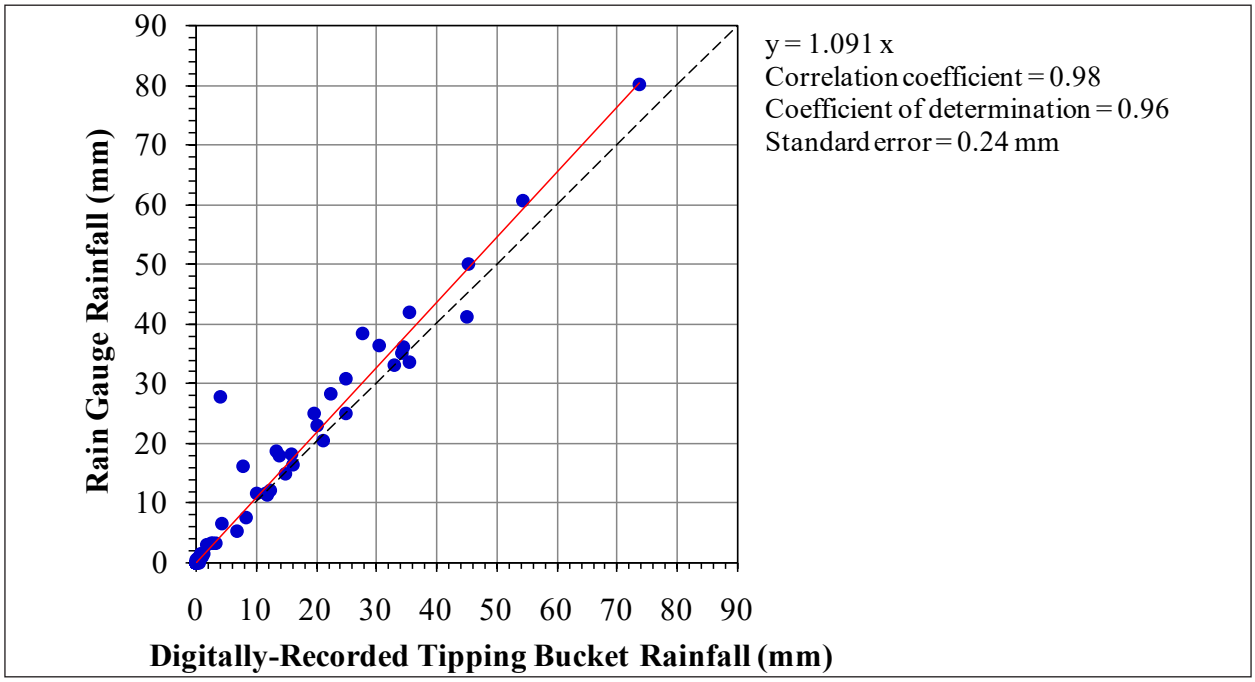

Fig. 1. Scatter plot between daily totals of rainfall recorded by digital rainfall recorder and ordinary rain gauge situated in study area. Firm line indicates linear trend line and broken line indicates 1:1 line

Determining Characteristics of Rainfall Storms: Storm-wise rainfall data at 1 min resolution were utilized to capture information and characterize the individual storms. Any two consecutive storms were distinguished based on the criterion that there was no rainfall for more than 6 h after cessation of the first storm (Wischmeier and Smith, 1978). Intensity and cumulative amounts of rainfall were computed over every 1 min temporal resolutions and the same were plotted for all rainfall storms occurring in the two years.

Computation of Rainfall Intensity, Rainfall Erosivity and Erosivity Density: The 1 min rainfall data were aggregated for each storm at D_t = 5, 15, 30 and 60 min and 24 h and the maximum 30 min rainfall intensity, I_{30} (mm h^{-1}), the total storm kinetic energy, E (MJ ha^{-1}), and storm erosion index or rainfall erosivity factor, EI_{30} (MJ mm ha^{-1} h^{-1}), were calculated for each D_t value (D_t = 5, 15, 30 and 60 min and 24 h).

The maximum 30 min (0.5 h) rainfall intensity, I_{30} (mm h^{-1}), for rainfall data was calculated as (Foster *et al*., 1981):

$$I_{30}=P_{30} / (0.5\ h) \quad ...1$$

where, P_{30} = maximum 30 min rainfall depth (mm).

The original, discontinuous unit energy equation was applied to calculate e (MJ ha^{-1} mm^{-1}) (Wischmeier and Smith, 1978):

$$e = 0.119+0.0873\ log\ I_{30} \quad I_{30} < 76\ mm\ h^{-1} \quad ...2$$

$$e=0.283 \quad I_{30} > 76\ mm\ h^{-1} \quad ...3$$

The unit energy (e) of individual storms was multiplied by their corresponding rainfall depths (P) to compute total kinetic energy E (MJ ha^{-1}) of that storm.

$$E=e\times P \quad ...4$$

Erosivity density (ED) is an important factor, defined as ratio of R-factor to rainfall amount (P), calculated on monthly or annual time interval (Kinnell, 2010). The ED, expressed in MJ ha^{-1} h^{-1}, is computed by the following expression.

$$ED_i=R_i / P_i \quad ...5$$

where, *EDi* = erosivity density value for i^{th} month, R_i = rainfall erosivity value for i^{th} month and *P* = rainfall amount for i^{th} month.

***Computation of Conversion Factors*:** In this study, values of I_{30}, E and R-factor calculated from 1 min resolution rainfall data were considered as the true or actual values. However, rainfall data at 1 min resolution are usually not available for most of the places/ regions all over the world. Hence, few of the previous studies from different parts of the world attempted to develop relationships for I_{30}, EI_{30} and R-factor values estimated from the fixed-rainfall data and their values obtained from high-resolution data. The results revealed a good linear relationship between values estimated using t min and 1 min values although the EI_{30} and R values were underestimated from t-min resolution rainfall data (e.g., Williams and Sheridan, 1991; Yin *et al*., 2007; Yue *et al*., 2020). Thus, in this study, conversion factors (CF_{Rt}) for R-factor were computed for the arid region, for the first time, to relate $R_{t\text{-}min}$ values from using t-min (t = 5, 15, 30, and 60 min and 24 h) rainfall data with those using 1 min rainfall data by developing linear regression models (Yue *et al*., 2020).

$$R_{(1\text{-}min)}=CF_{Rt}\times R_{(t\text{-}min)} \text{ for underestimated values} \quad ...6$$

$$R_{(1\text{-}min)}=R_{(t\text{-}min)} / CF_{Rt} \text{ for overestimated values} \quad ...7$$

Similarly, this study involved calculation of the conversion factors for 0.5 h rainfall intensity (CF_{It}) and storm energy (CF_{Et}) using the following equations.

$$I_{30(1\text{-}min)}=CF_{It} \times I_{30(t\text{-}min)} \quad ...8$$

$$E_{(1\text{-}min)}=CF_{Et} \times E_{(t\text{-}min)} \quad ...9$$

This study further explored the conversion factors for I_{30}, EI_{30} and R-factor values estimated from all fixed-time interval data, i.e., 1 min to 24 h.

Evaluating Under-/Over-estimation and Accuracy of Conversion Factors: The calculated conversion factors (CF_{Rt}) were utilized for estimating the R-factors at 1 min resolution from 5 min to 24 h data. The relative change (%) in the values of R-factor computed from 1 min ($R_{1\text{-}min}$) and other resolutions' data was used to examine under(over)-estimations of the R-factor values.

$$Relative\ error\ (\%)=((R_{(1\text{-}min)}-R_{(t\text{-}min)})/(R_{(1\text{-}min)}))\times 100 \quad ...10$$

The accuracy of the conversion factors (CF_{Rt}) for estimating R-factors using fixed interval rainfall data {t = 5, 15, 30 and 60 min and 24 h} was evaluated by using two performance criteria, i.e., symmetric mean

absolute percentage error (sMAPE) and Nash-Sutcliffe efficiency (NSE) (Yue *et al.*, 2020).

$$sMAPE\ (\%) = \frac{1}{n}\sum_{i=1}^{n}\left|\frac{R_{fi} - R_{hr}}{(R_{fi} + R_{hr})/2}\right| \times 100 \quad ...11$$

$$NSE = 1 - \frac{\sum_{i=1}^{n}(R_{fi} - R_{hr})^2}{\sum_{i=1}^{n}(R_{hr} - \overline{R_{hr}})^2} \quad ...12$$

Results and Discussion

Characteristics of Rainfall Storms: Over the two years (2020 and 2024), rainfall intensity and duration for a total of 21 erosive storms were recorded at 1 min resolution in the study area that could generate runoff to flow in the agricultural fields. The rainfall amount of such storms varied from 11.4 to 72.8 mm and duration ranged from 26 min to 8 h 56 min. The average rainfall intensity of the storms varied from 4.14 to 48.46 mm h^{-1}. The maximum intensity of rainfall for 30 min duration ranged from 11.6 to 50.0 mm h^{-1} in 2020 and from 12.8 to 86.0 mm h^{-1} in 2024. Bar charts of the rainfall intensity and line diagram of cumulative rainwater at 1 min resolution for those storms that had the maximum 30 min rainfall intensity (I_{30}) of 30 mm h^{-1} or more are depicted in Figs. 2 and 3

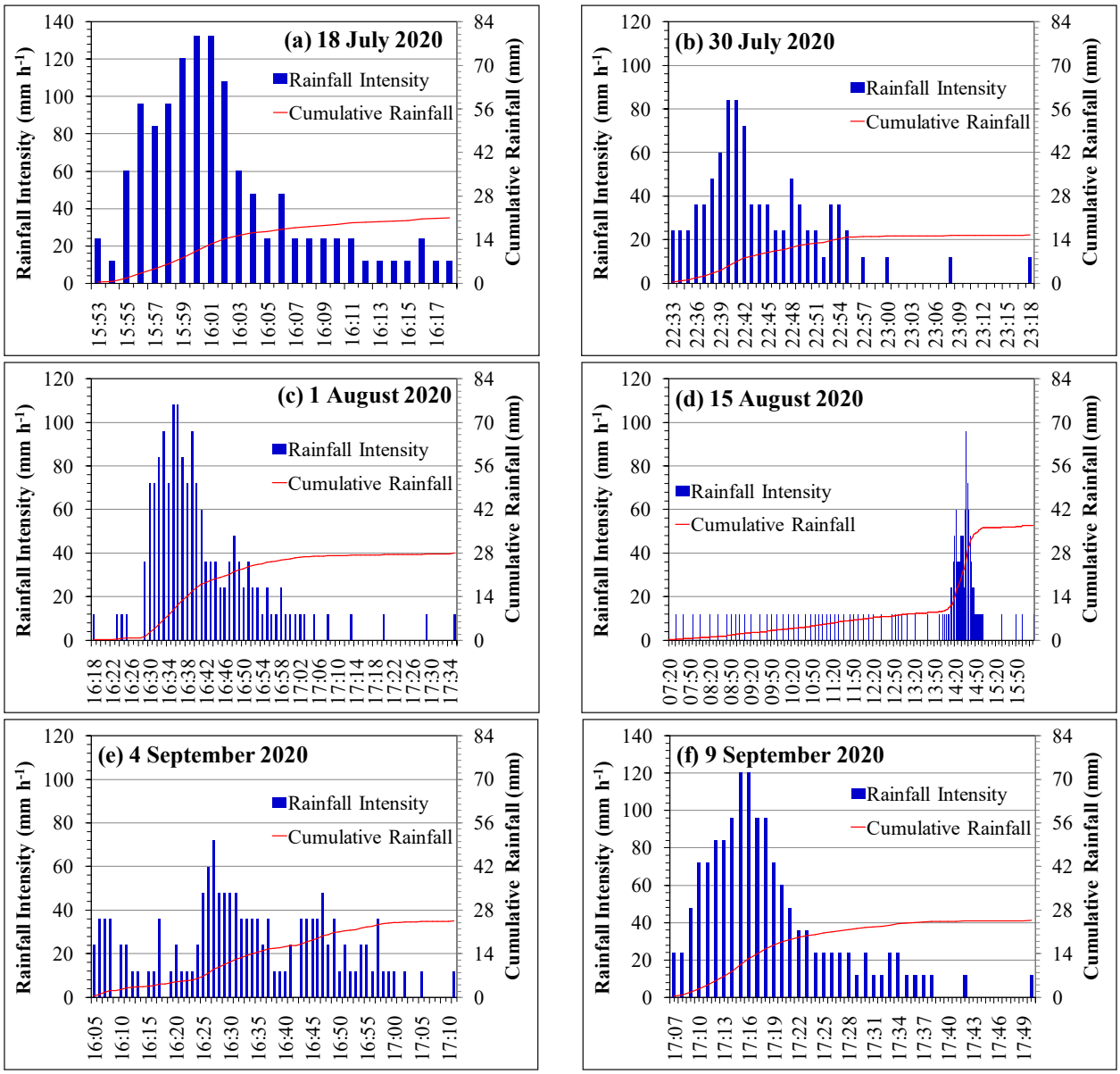

Fig. 2. Rainfall intensity and cumulative rainfall plotted for 1 min interval over the period of all rainfall storms that experienced the maximum 30 min rainfall intensity of more than 30 mm h-1 during 2020.

for the years 2020 and 2024, respectively. It is seen that six erosive storms of $I_{30} \geq 30$ mm h^{-1} occurred in 2020 (Fig. 2a-f) and five were witnessed in 2024 (Fig. 3a-e). It is seen that three storms in 2020 (Figs. 2a,c,f) and none in 2024 (Fig. 3a-e) attained the maximum rainfall intensity of more than 100 mm h^{-1} at 1 min resolution.

***Intensity, Rainfall Erosivity Factor and Erosivity Density*:** Using the 1 min resolution rainfall dataset, the maximum 30 min (0.5 h) intensity (I_{30}), unit kinetic energy (e) and total kinetic energy (E) were estimated for the individual storms; statistical summary of I_{30}, e, and E values are given in Table 1. It is seen that value of e ranged from 4.08 to 29.94 MJ ha^{-1} mm^{-1}, whereas E values of the rainfall storms varied from 2.49 to 19.84 MJ ha^{-1}. It is observed that E depends on the P_{30} as the maximum value of E does not coincide with the highest value of e rather it depends on the value of P_{30}.

The values of the rainfall erosivity factor (R) ranged from 30.038 to 1706.420 MJ mm ha^{-1} h^{-1} with the mean value of 259.689 MJ mm ha^{-1} h^{-1} (Table 1). The standard deviation for R values (362.930 MJ mm ha^{-1} h^{-1}) is found more than its mean value, which indicates large variation with 140% of coefficient of variation (CV). Value of the erosivity density for rainfall storms of arid region ranged from 2.546 to 23.440 MJ ha^{-1} h^{-1} with the mean and standard deviation of 8.422 and 4.794 MJ ha^{-1} h^{-1}, respectively (Table 1).

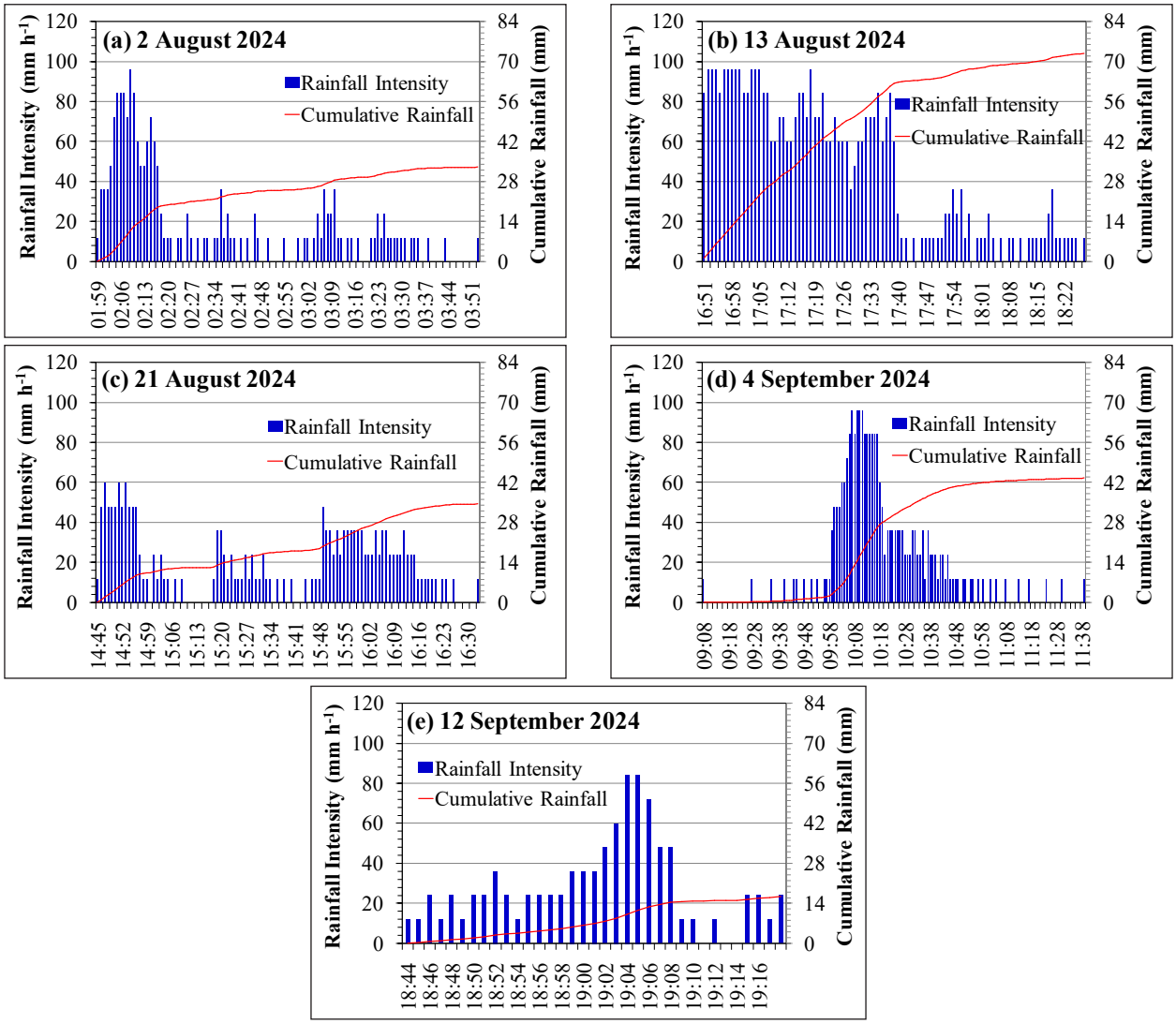

Fig. 3. Rainfall intensity and cumulative rainfall plotted for 1 min interval over the period of all rainfall storms that experienced the maximum 30 min rainfall intensity of more than 30 mm h-1 during 2024

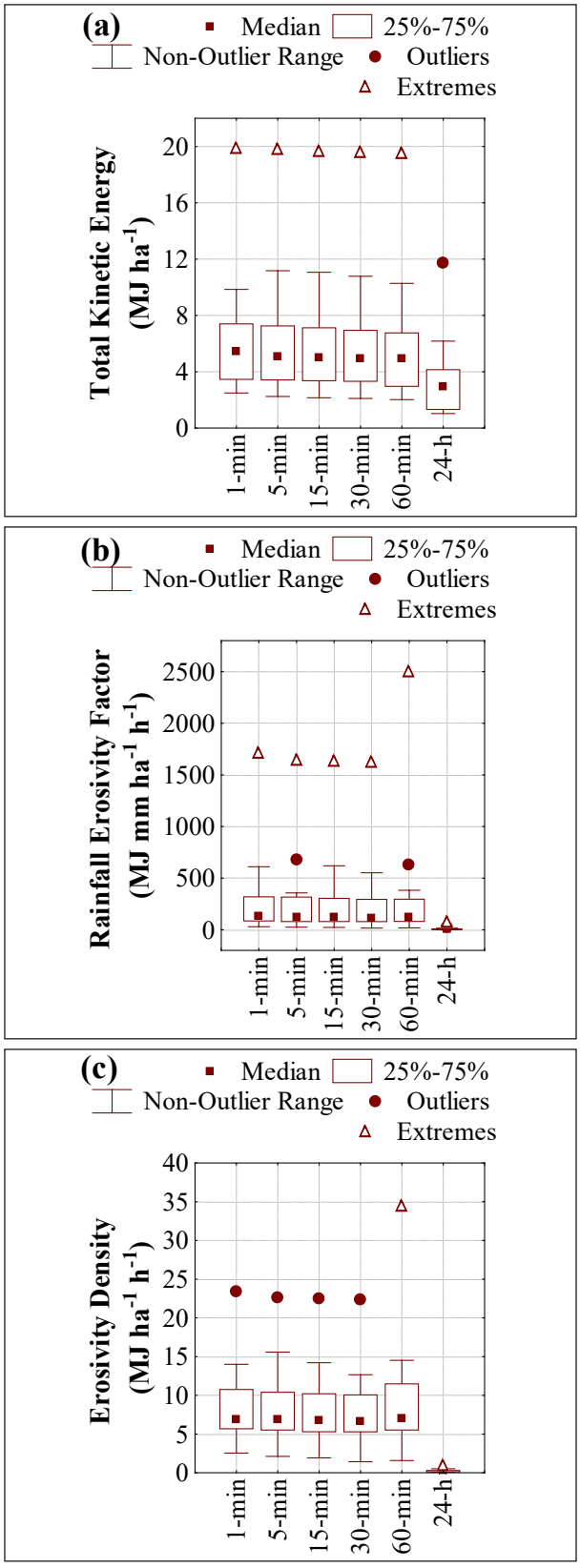

Fig. 4. Box-whisker plots of (a) total kinetic energy, (b) rainfall erosivity factor and (c) erosivity density computed from 1 min resolution rainfall data.

Thus, the CV is 57% for the ED, which indicates high variation (CV>30%) among the values.

The parameters E, R and ED were also computed at 5 min, 15 min, 30 min, 60 min and 24 h resolutions using the rainfall dataset aggregated from rainfall monitored at 1 min resolution. Distribution of the values of E, R and ED at different temporal resolutions is shown by drawing box-whisker plots as depicted in Figs. 4(a-c). It is seen that the median values of total kinetic energy (E_{med}) decreases on making temporal resolution of rainfall measurement coarser from 1 min (E_{med} = 5.5 MJ ha^{-1}) to 60 min (E_{med} = 4.9 MJ ha^{-1}), and it further reduced up to 3 MJ ha^{-1} for further coarser resolution of 24 h (Fig. 4a). However, medians of R-factor reduced only up to 116.2 MJ mm ha^{-1} h^{-1} at coarser resolution of 30 min from 128.5 MJ mm ha^{-1} h^{-1} at 1 min resolution. The R_{med} value increased at 60 min resolution and then drastically decreased to 4.2 MJ mm ha^{-1} h^{-1} for 24 h resolution (Fig. 4b). Similarly, median values of erosivity density (ED_{med}) showed a reduction from 1 min (6.9 MJ ha^{-1} h^{-1}) to 30 min (6.6 MJ ha^{-1} h^{-1}) resolution, then it increased at 60 min (7.0 MJ ha^{-1} h^{-1}) resolution and decreased considerably at 24 h resolution (ED_{med} = 0.2 MJ ha^{-1} h^{-1}) (Fig. 4c).

Underestimation/Overestimation of Total Energy, R-Factor and Erosivity Density: The values of the unit energy (e) and total energy (E), R-factor and erosivity density computed for 5 to 60 min and 24 h were compared with that estimated at 1 min resolution (Table 2). In general, the unit kinetic energy computations revealed continuously increasing underestimations from 5 min (-71.8%), 15 min (-89.5%), 30 min (-94.5%), 60 min (-96.9%) and 24 h (-98.9%) rainfall data, respectively. Following the similar pattern, underestimations for total kinetic energy increased on increasing temporal resolution from 5 min to 60 min with relative error within -10%; however, a considerable underestimation for the total kinetic energy (-46%) was observed from 24 h rainfall data. The similar pattern was observed in case of R-factor where underestimations were -4.5, -8.0, -9.6, -5.8 and -96.7% from 5, 15, 30 and 60 min and 24 h, respectively (Table 2). Likewise, the underestimations for erosivity density increased from 5 to 30 min, then slight overestimation (5%) from 60 min rainfall data

Table 1. Kinetic energy, rainfall erosivity factor and erosivity density of rainfall storms recorded at 1 min interval in Indian arid region

S. No.	Storm Date	Rainfall depth (mm)	Storm duration (min)	Maximum 30 min rainfall intensity (mm h^{-1})	Unit kinetic energy (MJ ha^{-1} mm^{-1})	Total kinetic energy (MJ ha^{-1})	Rainfall erosivity factor (MJ mm ha^{-1} h^{-1})	Erosivity density (MJ Ha^{-1} h^{-1})
1	18-Jul-20	21	26	42.0	6.47	5.66	237.761	11.322
2	30-Jul-20	15.6	45	30.4	6.67	4.03	122.578	7.858
3	1-Aug-20	28	77	50.0	10.94	7.40	369.955	13.213
4	15-Aug-20	37	536	43.2	23.43	9.02	389.841	10.536
5	3-Sep-20	11.8	164	11.6	11.27	2.59	30.038	2.546
6	4-Sep-20	24.6	66	32.4	13.08	6.13	198.624	8.074
7	6-Sep-20	20	137	24.0	12.80	4.85	116.451	5.823
8	7-Sep-20	13.6	27	27.2	6.52	3.46	94.022	6.913
9	9-Sep-20	24.8	43	48.0	8.45	6.64	318.815	12.855
10	14-9-20	12.2	34	23.6	6.16	3.09	73.009	5.984
11	2-Aug-24	33.2	113	42.4	17.42	8.42	357.071	10.755
12	4-Aug-24	25.4	111	20.8	15.53	6.18	128.471	5.058
13	5-Aug-24	25.2	221	14.8	25.18	5.47	80.920	3.211
14	13-Aug-24	72.8	100	86.0	22.52	19.84	1706.420	23.440
15	15-Aug-24	15	59	24.0	10.44	3.55	85.244	5.683
16	21-Aug-24	34.6	107	29.2	24.52	7.53	219.764	6.352
17	25-Aug-24	12.8	29	25.6	4.08	3.46	88.647	6.926
18	31-Aug-24	11.4	124	12.8	11.03	2.49	31.919	2.800
19	2-Sep-24	11.4	27	22.8	6.19	2.82	64.393	5.649
20	4-Sep-24	43.6	151	62.0	29.94	9.85	610.576	14.004
21	12-Sep-24	16.4	34	30.8	7.73	4.19	128.956	7.863
Range		11.4-72.8	26-536	11.6-86.0	4.08-29.94	2.49-19.84	30.038-1706.420	2.546-23.440
Mean		24.30	106.24	33.50	13.35	6.03	259.689	8.422
Standard deviation		14.53	112.34	17.67	7.60	3.85	362.930	4.794
Coefficient of variation (%)		60	106	53	57	64	140	57

and considerable underestimation (-97.1%) from 24 h rainfall data were observed.

Conversion Factors for the R-Factor: Scatter plots between $R_{t\text{-}min}$ factor computed from t-time rainfall data (t = 5, 15, 30 and 60 min, 24 h) and $R_{1\text{-}min}$ factor computed from 1 min rainfall data are depicted in Fig. 5. Values of the coefficient of determination, ranging from 0.951 to 0.997, indicated excellent linear regressions. The values of conversion factors increased from 1.019 to 1.064 on increasing time interval (t) from 5 to 30 min, and then CF_{Rt} decreases to 0.727 on increasing the interval up to 60 min. On increasing the time interval to 24 h, CF_{Rt} rises drastically to 24.75 (Fig. 5e). The deviation of the fitted linear trend line from the 1:1 line increased with the increasing time interval from 5 to 30 min, which revealed an increasing underestimation of R-factor with rising time interval (Fig. 5a-c). Divergence of the trend line from 1:1 line further indicates overestimation of R-factor at time interval of 60 min, and a considerable underestimation at 24 h. It is further observed that the R-factor less than 400 MJ mm ha^{-1} h^{-1} were not much underestimated from the data of time interval within 15 min; however, the R-factor for storm with higher erosivity were underestimated up to 30 min interval and overestimated at 60 min data interval. The considerable underestimation/ overestimation were likely responsible for the statistically-significant (α = 0.05) differences found in R-factor values on comparing the values obtained from 5 min to 24 h with those

Table 2. Relative error incurred in estimating kinetic energy, erosivity factor and erosivity density from 5 to 60 min and 24 h rainfall data

Temporal resolution	Relative error (%)			
	Unit kinetic energy (e)	Total kinetic energy (E)	Rainfall erosivity factor (R)	Erosivity density (ED)
5 min	-71.8	-7.6	-4.5	-1.3
15 min	-89.5	-8.6	-8.0	-2.8
30 min	-94.5	-9.5	-9.6	-4.1
60 min	-96.9	-10.4	-5.8	0.5
24 h	-98.9	-46.0	-96.7	-97.1

estimated from 1 min data by applying paired t-test.

The values of the conversion factors for R-factors from 5 min to 24 h data are given in Table 3 along with values of the two performance criteria, i.e., sMAPE and NSE. It is seen that NSE values of the regression models are above 0.99 for 5 to 30 min data and are 0.75 for 60 min and -0.42 for 24 data. However, the NSE improved for R-factor values converted from 5 min to 24 h data to those estimated through 1 min data. Similarly, values of sMAPE decreased after the conversion by 1%, 3%, 4% and 130% for the 5 min, 15 min, 30 min and 24 h data though it showed 12% increase for 60 min data. This finding suggested that the obtained conversion factors (CF_{Rt}) are effective in converting R-factor values based on coarser resolution of 5 min time interval or more to those from 1 min data.

Conversion Factors for I_{30} and E: The results of the linear regression analysis revealed that the values of I_{30} computed at finer resolutions using coarser time resolution rainfall data showed a significant positive relationship from 5 to 30 min data as R^2 values are more than 0.90 (Fig. 6a). However, I_{30} values computed from 60 min (R^2 ~ 0.843-0.860) and 24 h (R^2 ~ 0.647-0.675) fixed interval data did not depict strong relationships. On the other hand, the values of E and R-factor computed at finer resolution from fixed 5 min to 24 h interval rainfall data indicated strong linear relationships with R^2 values greater than 0.90 (Fig. 6a). Values of slope (b) indicating conversion factors (CF_{It}) of the linear regression models were found to be more than 1.0 for I_{30} computed at finer resolution from 5 to 30 min data, which indicated underestimations; however, I_{30} were overestimated at finer resolution from 60 min data and highly underestimated from 24 h data (Fig. 6b). In case of E, values of CF_{Et} were found to be greater than 1.0 for E values calculated at finer resolution from 5 min to 24 h data although the values estimated from 24 h data were highly underestimated. Similar to the I_{30}, computation of the R-factor revealed underestimations (CF_{Rt}>1.0) at finer resolution from 5 to 30 min data; the R-factors computed at finer resolution from 60 min data revealed overestimations (CF_{Rt}<1.0) and highly underestimated from 24-data (Fig. 6b).

The ratios of the conversion factors for 1 min interval to other time intervals are plotted over the time interval (Fig. 7a). It is seen that the values for I_{30}, E and R-factor decreased from 5 min to 24 h with spike in the values of I_{30} and R-factor at 60 min time interval. It is obvious that the presence of spike at 60 min interval for I_{30} and R-factor was responsible for the poor linear regression between the ratios and

Table 3. Conversion factors for estimating rainfall erosivity (R factor) at 1 min time interval using rainfall data measured at higher time intervals

	5 min	15 min	30 min	60 min	24 h
Conversion factor	1.019	1.043	1.064	1.340	24.75
sMAPE[a]	5.5%	8.0%	13.4%	17.3%	188.1%
NSE[a]	1.00	0.99	0.99	0.75	-0.42
sMAPE[b]	4.3%	5.8%	9.1%	29.2%	49.1%
NSE[b]	1.00	1.00	1.00	-0.10	0.95

Note: sMAPE - symmetric mean absolute percentage error; NSE – Nash-Sutcliffe Efficiency; [a] indicates before conversion; [b] indicates after conversion

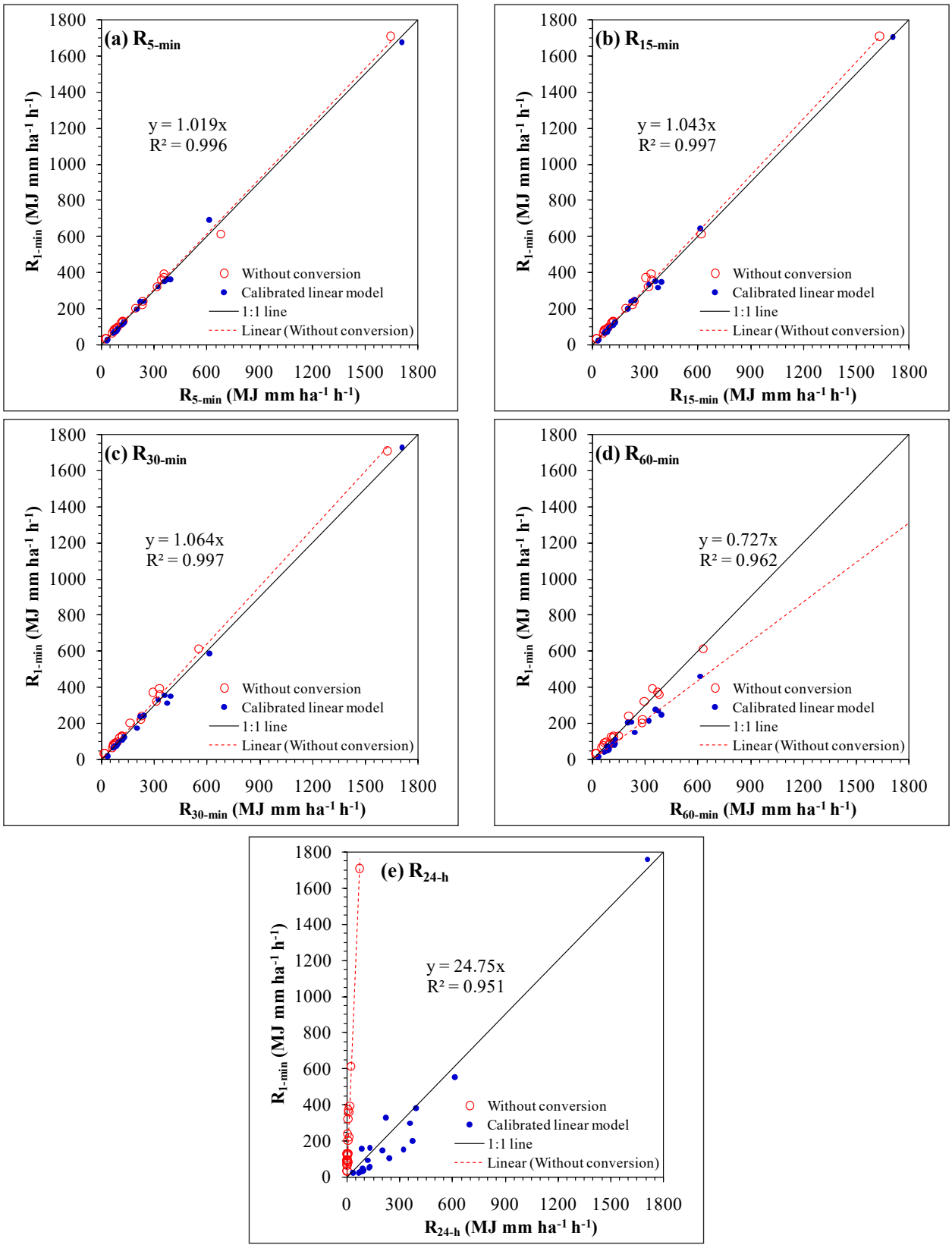

Fig. 5. Regression models of rainfall erosivities estimated from 5 min to 24 h data. The dotted line represents the calibrated linear model. The circles are R factors estimated from 5 to 60 min data without conversions. The dots are values multiplied by conversion factors

time intervals (R^2<0.50) (Fig. 7a). On removing the single point at 60 min interval, the linear relationship improved especially for I_{30} (R^2 = 0.632) and R-factor (R^2 = 0.635) (Fig. 7b).

Of the total storms considered in this study, the maximum 30 min rainfall intensity (I_{30}) was high (18-30 mm h^{-1}) for 38% storms, very high (30-60 mm h^{-1}) for 38% storms and severe

Fig. 6. Cross relationships for I30, E and R-factor among different time intervals showing (a) coefficient of determination (R2), and (b) slope values of linear equations

(>60 mm h^{-1}) for 10% storms; I_{30} of only 14% storms was low (<18 mm h^{-1}), according to the intensity classification criterion, reported in Singh and Singh (2020). Furthermore, following the intensity classification proposed for the tropical countries like India (Striffler *et al.*, 1979), the rainfall intensity was moderate (15.1-40 mm h^{-1}) for 52% storms, heavy (40.1-70 mm h^{-1}) for 29% storms, and severe (70-100 mm h^{-1}) for 5% storm; only 14% storms depicted gentle intensity (<15 mm h^{-1}). This suggests that intensity (I_{30}) of 75-80% of the rainfall storms

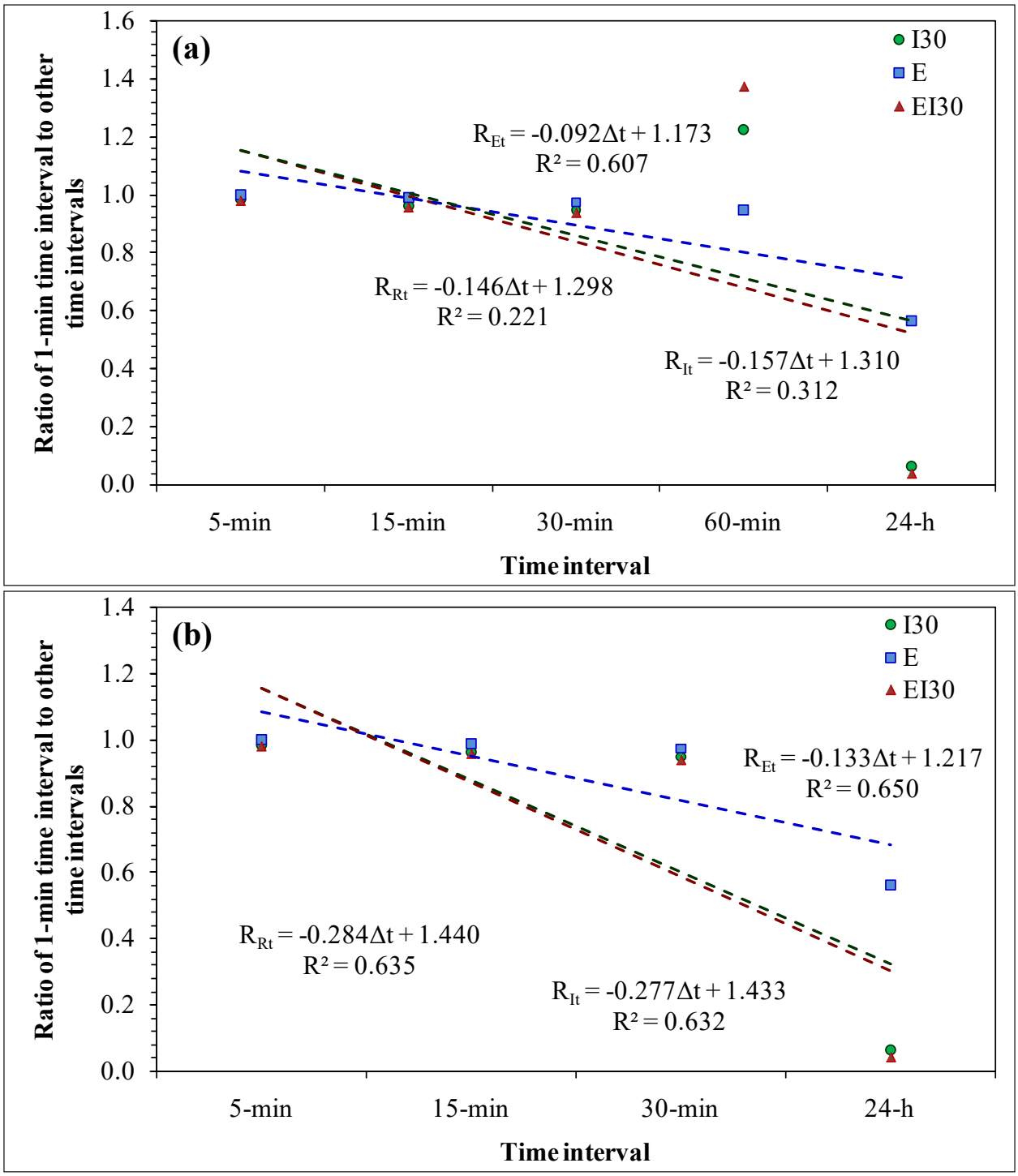

Fig. 7. Ratios of the conversion factors for I30, E and EI30 estimated from 5 min to 24 h time interval to that estimated at 1 min interval for (a) whole time intervals, and (b) excluding 60 min time interval.

in the study area, situated in arid climate, was high (moderate) to very high (heavy) and even 5-10% storms were of severe intensity. The recent increase in the rainfall intensity seems to be a new normal for the Indian arid region, which may intensify the problems of soil erosion especially from the agricultural lands. Furthermore, there is adequate scope of implementing rainwater harvesting structures to get rid of huge runoff water flowing over the crop fields, and utilizing the stored rainwater for improving agricultural productivity of the drylands.

Results of this study revealed that as the rainfall measurement interval decreases from 30 to 1 min, value of I_{30}, E and R-factor increase. This finding is found in agreement with results of earlier studies reported from different parts of the world. For example, Porto (2016) reported that increase in values of EI on decreasing the time interval from 60 to 5 min in Calabria, southern Italy. Similarly, in western Oregon of the United States, Istok *et al*. (1986) ascertained 19.3% to 37.8% increase in EI values on decreasing time interval of rainfall measurement from 60 to 15 min. Likewise, Tu *et al*. (2023) explored the effect of time interval on rainfall erosivity and observed that both E and I_{30} increased when time interval decreased although declining rate was faster for I_{30}. The decrease in R-factor on increasing the measurement interval of rainfall data is mainly caused due to decrease in I_{30} (Tu *et al*., 2023). In arid climate of the study area, it is experienced that the rainfall intensity remains the maximum for a period of much less than 30 min, and its distribution over the whole storm's period remains less towards the end. Thus, on increasing the time interval, the I_{30} value starts diminishing, which in-turn decreases the EI or R values. On the other hand, on reducing the time interval for rainfall measurement, the peaks of the very high to severe rainfall intensity are adequately captured, and thus, finer temporal resolution up to 1 min escalates the rainfall intensity as well as erosive energy of the rainfall storms.

The equations developed originally for computation of rainfall erosivity (EI_{30} or R-factor) involved rainfall data for the breakpoints that was conventionally determined from the graphs/ charts of automatic rain gauges. However, with the advancement of the technology, use of fixed time-interval data, generated digitally through rainfall recorders and automatic weather stations following tipping-bucket mechanism and recorded by data loggers, has broadened. Hence, the fixed time-interval data for the different periods such as 15 min, 30 min, 60 min etc. started being used customarily in rainfall erosivity computations (Panagos *et al*., 2016; Tu *et al*., 2023; Yin *et al*., 2007; Yue *et al*., 2020). It is further observed that at finer time resolutions of rainfall monitoring, the accuracy of erosivity computations gets improved as value of rainfall intensity starts diminishing gradually on increasing time resolution (Dunkerley, 2019). Similar to the findings of Tu *et al*. (2023), both E and I_{30} decreased in this study on increasing the value of time interval, except at time interval of 60 min. It is further revealed that the value of I_{30} decreased faster than that of E, which is responsible for the decrease in the value of R-factor (Yin *et al*., 2007; Tu *et al*., 2023). Also, finding breakpoints in the previously used graphs of rain gauges were difficult, subjective sometimes and time-consuming (Tu *et al*., 2023). Non-availability of the rain gauge records for the historical times is another drawback associated with use of breakpoint rainfall data (Beguería *et al*., 2018).

The conversion factors for the different parts of the world are enlisted in Table 4. It is seen that earlier studies reported conversion factors mostly for the humid and semi-arid regions at time interval of 5 min, 6 min, 10 min, 15 min, 30 min and 60 min for monitoring of rainfall. Unlike to the conventional studies, this study determined the conversion factors for the arid region of India and included 24 h time interval for rainfall measurement. Also, this study determined the factors based on E, I_{30} and R-factor (EI_{30}) indexes. It is revealed that the values of the conversion factors are obtained less for the arid region in comparison to that reported for the humid and semi-arid regions. It is further revealed that the conversion factors for 24 h time interval are of much higher magnitude than that computed for the less than 60 min interval. In general, values of the R-factor are underestimated on increasing the time interval of rainfall measurement (Yue *et al*., 2020). However, in this study, conversion factors have been computed satisfactorily based on strong relationships between the R-factor estimations based on 1 min time interval and

Table 4. Conversion factors (CFs) for converting EI30 (R factor) values from 5 to 60 min rainfall data to values estimated from high-resolution data

Country	Study area	Climate	5 min	6 min	10 min	15 min	30 min	60 min	24 h	Resolution of data compared	Index	Reference
United States	Western Oregon	Humid	–	–	–	–	–	1.193-1.378	–	15 min	EI_{30}	Istok *et al.* (1986)
United States	South-eastern Georgia	Humid	1.0416	1.0405	1.09	1.1209	1.3127	1.837	–	Breakpoint	EI_{30}	Williams and Sheridan (1991)
United States	Eastern part	Humid	–	–	–	–	–	1.08-3.16	–	15 min	EI_{30}	Renard (1997)
Italy	Sicily	Semi-arid	–	–	–	–	–	1.33	–	15 min	EI_{30}	Agnese *et al.* (2006)
China	Eastern China	Humid	1.014 (1.010-1.020)	–	1.044 (1.023-1.069)	1.078 (1.039-1.114)	1.161 (1.094-1.257)	1.73 (1.568-1.814)	–	Breakpoint	EI_{30}	Yin *et al.* (2007)
Europe		Humid and semi-arid	0.7984 (0.7514-0.8568)	–	0.8205 (0.7986-0.8951)	0.8716 (0.8072-0.9233)	1	1.5597 (1.2974-1.6995)	–	30 min	R factor	Panagos *et al.* (2015); (2016)
Italy	Calabria	Humid	0.92		0.97		1.12	1.53	–	15 min	EI_{30}	Porto (2016)
China	Mainland	Humid, semi-arid, arid	1.051	1.058	1.083	1.121	1.253	1.871	–	1 min	R factor	Yue *et al.* (2020)
China	Mainland	Humid, semi-arid, arid	1.034	1.044	1.053	1.090	1.180	1.489	–	1 min	R factor 1-in-10-year EI_{30}	Yue *et al.* (2020)
China	Dean County, Jiangxi Province	Humid	1.05	–	1.09	1.12	1.21	1.95	–	1 min	EI_{30}	Tu *et al.* (2023)
India	Western Rajasthan	Arid	1.019	–	–	1.043	1.064	0.727	24.75	1 min	R factor	This study
India	Western Rajasthan	Arid	0.997	–	–	1.009	1.025	1.055	1.776	1 min	E	This study
India	Western Rajasthan	Arid	1.016	–	–	1.038	1.055	0.816	15.51	1 min	I_{30}	This study

other coarser time intervals that are mostly used for the rainfall monitoring. Hence, the developed relationships can effectively be used for estimating the actual and accurate E, I_{30} and R-factor values. The conversion factors for the precise computations of the parameters are not available for any part of India, and thus, this is the first study, where such factors are determined, for the first time, for arid region of India.

Conclusions

This study determined conversion factors for estimating rainfall intensity (I_{30}), kinetic energy (E) and erosivity (R-factor) at 1 min resolution from rainfall data measured at fixed time intervals such as 5 min, 15 min, 30 min, 60 min and 24 h. Unlike the previous studies reported from humid and semi-arid regions, this study attempted to develop the conversion factors for arid region, for the first time, by measuring rainfall occurrences at 1 min interval in India. The results indicated the occurrence of highly erosive rainfall storms with the peak intensity of 75 mm h^{-1} or more in the recent years. In spite of the fact that soil type is sandy loam in the study area having the basic infiltration rate of 30 mm h^{-1}, huge runoff quantities have been generating in the area for the last few years in response to high intensity rainfall storms. The maximum 30 min rainfall intensity (I_{30}) of most of the storms exceeded the soil infiltration rate, and thus, the kinetic energy (E) is so high that the soils are always at the risk of erosion. The value of R-factor (30.038-1706.420 MJ mm ha^{-1} h^{-1}) and erosivity density (ED) (2.546-23.440 MJ ha^{-1} h^{-1}) depicted a large temporal variability (coefficient of variation, CV>30%) indicating uncertainty in intensity, magnitude and duration of rainfall occurrences. On making the time interval further coarser (5 min, 15 min, 30 min, 60 min and 24 h), both the R-factor and ED decreased up to 30 min, increased at 60 min and drastically reduced at 24 h. In general, on increasing time interval of rainfall measurement from 5 to 60 min, values of E, R-factor and ED showed under(over)-estimations within 10%; however, at 24 h interval, the underestimations were considerably high (46%-97%).

The values of the conversion factors for the R-factor ranged from 1.019 to 1.604 for the time interval from 5 min to 30 min and showed an abrupt rise up to 24.75 for 24 h interval. The computed conversion factors may be utilized for converting values of I_{30}, E and R-factor estimated from 5 min or coarser time intervals to 1 min high-resolution interval precisely as revealed by the high values of the coefficient of determination (R^2>0.95). The accuracy of the conversion factors is further confirmed with improved values of Nash-Sutcliffe efficiency (NSE) and systematic mean absolute percentage error (sMAPE). The I_{30} values computed at finer resolution rainfall revealed significant relationships (R^2>0.90) with those computed by using coarser resolution data up to 30 min time interval; R^2 values were less than 0.86 for 60 min and 0.67 for 24 h data. Therefore, it is suggested to use rainfall measurements up to the highest interval of 30 min for precise computations of I_{30}, E and R-factor.

Acknowledgements

The authors are grateful to the Director, ICAR-Central Arid Zone Research Institute, Jodhpur for providing necessary facilities to carry out this study.

Data availability statement

Data will be provided by the corresponding author on receiving a reasonable request.

References

Agnese, C., Bagarello, V., Corrao, C., D'Agostino, L. and D'Asaro, F. (2006). Influence of the rainfall measurement interval on the erosivity determinations in the Mediterranean area. *Journal of Hydrology* 329(1-2): 39-48. https://doi.org/10.1016/j.jhydrol.2006.02.002

Beguería, S., Serrano-Notivoli, R. and Tomas-Burguera, M. 2018. Computation of rainfall erosivity from daily precipitation amounts. *Science of the Total Environment* 637: 359-373. https://doi.org/10.1016/j.scitotenv.2018.04.400

Bhattacharyya, R., Ghosh, B.N., Mishra, P.K., Mandal, B., Rao, C.S., Sarkar, D., Das, K., Anil, K.S., Lalitha, M., Hati, K.M., ***et al***. 2015. Soil degradation in India: Challenges and potential. *Sustainability* 7: 3528-3570. https://doi.org/10.3390/su7043528

Diodato, N., Borrelli, P., Fiener, P., Bellocchi, G. and Romano, N. 2017. Discovering historical rainfall erosivity with a parsimonious approach: A case study in Western Germany. *Journal of Hydrology* 544: 1-9. https://doi.org/10.1016/j.jhydrol.2016.11.023

Dunkerley, D. 2019. How does sub-hourly rainfall intermittency bias the climatology of hourly and daily rainfalls? Examples from arid and wet tropical Australia. *International Journal*

of Climatology 39(4): 2412-2421. https://doi.org/10.1002/joc.5961

Fiener, P., Neuhaus, P. and Botschek, J. 2013. Long-term trends in rainfall erosivity-analysis of high-resolution precipitation time series (1937-2007) from Western Germany. *Agricultural and Forest Meteorology* 171-172(8): 115-123. https://doi.org/10.1016/j.agrformet.2012.11.011

Foster, G.R., McCool, D.K., Renard, K.G. and Moldenhauer, W.C. 1981. Conversion of the universal soil loss equation to SI metric units. *Journal Soil and Water Conservation* 36(6): 355-359. https://doi.org/10.1080/00224561.1981.12436140

Hanel, M., M_aca, P., Ba_sta, P., Vlnas, R. and Pech, P. 2016. The rainfall erosivity factor in the Czech Republic and its uncertainty. *Hydrology and Earth System Sciences* 20: 4307-4322. https://doi.org/10.5194/hess-20-4307-2016

ICAR and NAAS 2010. Degraded and Wastelands of India - Status and Spatial Distribution. Indian Council of Agricultural Research (ICAR) and National Academy of Agricultural Sciences (NAAS), New Delhi, India, 158 p.

IPCC 2001. Climate Change 2001: The Scientific Basis. Working Group I, 2001, Contribution of Working Group I to the Third Assessment Report of the Intergovernmental Panel on Climate Change (IPCC), Cambridge University Press, Cambridge, United Kingdom.

IPCC 2007. Climate Change 2007: Impacts, Adaptation, and Vulnerability. In: *Contribution of Working Group II to the Fourth Assessment Report of the Intergovernmental Panel on Climate Change (IPCC)* (Eds. M. Parry, M.L. Parry, O. Canziani, J. Palutikof, P. Van der Linden and C. Hanson), pp. 470-506. Cambridge University Press, Cambridge, United Kingdom, pp. 470-506.

IPCC 2012. Seneviratne, S.I., Nicholls, N., Easterling, D., Goodess, C.M., Kanae, S., Kossin, J., Luo, Y., Marengo, J., McInnes, K., Rahimi, M., Reichstein, M., Sorteberg, A., Vera, C. and Zhang, X. Changes in climate extremes and their impacts on the natural physical environment. In: *Managing the Risks of Extreme Events and Disasters to Advance Climate Change Adaptation, A Special Report of Working Groups I and II of the Intergovernmental Panel on Climate Change (IPCC)* (Eds. Field, C.B. Field, V. Barros, T.F. Stocker, D., Qin, D.J. Dokken, K.L. Ebi, M.D. Mastrandrea, K.J. Mach, G.-K. Plattner, S.K. Allen, M. Tignor and P.M. Midgley), pp. 109-230. Cambridge University Press, Cambridge, United Kingdom, and New York, NY, USA.

Istok, J., McCool, D., King, L. and Boersma, L. 1986. Effect of rainfall measurement interval on EI calculation. *Transactions of the American Society of Agricultural Engineers* 29(3): 730-734. https://doi.org/10.1016/j.catena.2022.106714

Katsir, S., Biswas, A.K., Urs, K., Lenka, N.K., Jha, P. and Arora, K. 2024. Governing soils sustainably in India: Establishing policies and implementing strategies through local governance. *Soil Security* 14: 100132. https://doi.org/10.1016/j.soisec.2024.100132

Kinnell, P.I.A. 2010. Event soil loss, runoff and the universal soil loss equation family of models: A review. *Journal of Hydrology* 385: 384-397. https://doi.org/10.1016/j.jhydrol.2010.01.024

Klik, A., Haas, K., Dvorackova, A. and Fuller, I.C. 2015. Spatial and temporal distribution of rainfall erosivity in New Zealand. *Soil Research* 40(6): 887-901. http://dx.doi.org/10.1071/SR14363

Lal, R. 2012. Land degradation and pedological processes in a changing climate. *Pedologist* 55(3): 315-325. https://doi.org/10.18920/pedologist.55.3_315

Machiwal, D., Dayal, D. and Kumar, S. 2015. Assessment of reservoir sedimentation in arid region watershed of Gujarat. Journal of Agricultural Engineering, *ISAE* 52(4): 40-49. https://doi.org/10.52151/jae2015524.1590

Machiwal, D., Kumar, S. and Dayal, D. 2016. Characterizing rainfall of hot arid region by using time series modeling and sustainability approaches: A case study from Gujarat, India. *Theoretical and Applied Climatology* 124: 593-607. https://doi.org/10.1007/s00704-015-1435-9

Machiwal, D., Kumar, S., Dayal, D. and Mangalassery, S. 2017. Identifying abrupt changes and detecting gradual trends of annual rainfall in an Indian arid region under heightened rainfall rise regime. *International Journal of Climatology* 37(5): 2719-2733. https://doi.org/10.1002/joc.4875

Machiwal, D., Patel, A., Kumar, S. and Naorem, A. 2022. Status and challenges of monitoring soil erosion in croplands of arid regions. In: *Soil Health and Environmental Sustainability* (Eds. P.K. Shit, P.P. Adhikary, G.S. Bhunia, D. Sengupta),. Environmental Science and Engineering. Springer, Cham. https://doi.org/10.1007/978-3-031-09270-1_8

Mannaerts, C.M. and Gabriels, D. 2000. Rainfall erosivity in Cape Verde. *Soil and Tillage Research* 55(3): 207-212. http://dx.doi.org/10.1016/j.geoderma.2013.10.026

Martins, S.G., Avanzi, J.C., Silva, M.L.N., Curi, N., Norton, L.D. and Fonseca, S. 2010. Rainfall erosivity and rainfall return period in the experimental watershed of Aracruz, in the coastal plain of Espirito Santo, Brazil. *Revista Brasileira de Ciência do Solo* 34(3): 999-1004. http://dx.doi.org/10.1590/S0100-06832010000300042

McFarlane, D.J., Davies, R.J. and Westcott, T. 1986. Rainfall erosivity in Western Australia. In: Proceedings of the Hydrology and Water Resources Symposium, Griffith University, Brisbane. Institution of Engineers, Australia, Barton, ACT, pp. 350-354.

Meena, H.M., Machiwal, D., Santra, P., Moharana, P.C. and Singh, D.V. 2019. Trends and homogeneity of monthly, seasonal, and annual rainfall over arid region of Rajasthan, India. *Theoretical and Applied Climatology* 136: 795-811. https://doi.org/10.1007/s00704-018-2510-9

Meusburger, K., Steel, A., Panagos, P., Montanarella, L. and Alewell, C. 2012. Spatial and temporal variability of rainfall erosivity factor for Switzerland. *Hydrology and Earth System Sciences* 16: 167-177. https://doi.org/10.5194/hess-16-167-2012

NAAS 2012. Management of Crop Residues in the Context of Conservation Agriculture. Policy Paper No. 58, National Academy of Agricultural Sciences (NAAS), New Delhi, India, 12p.

Panagos, P., Ballabio, C., Borrelli, P., Meusburger, K., Klik, A., Rousseva, **S.,** *et al.* 2015. Rainfall erosivity in Europe. Science of the Total Environment, 511: 801-814. https://doi.org/10.1016/j.scitotenv.2015.01.008

Panagos, P., Borrelli, P., Spinoni, J., Ballabio, C., Meusburger, K., Beguería, S., Rousseva, S., *et al*. 2016. Monthly rainfall erosivity: Conversion factors for different time resolutions and regional assessments. *Water* 8(4): 119. https://doi.org/10.3390/w8040119

Porto, P. 2016. Exploring the effect of different time resolutions to calculate the rainfall erosivity factor R in Calabria, southern Italy. *Hydrological Processes* 30(10): 1551-1562. https://doi.org/10.1002/hyp.10737

Renard, K.G. 1997. Predicting soil erosion by water: A guide to conservation planning with the Revised Universal Soil Loss Equation (RUSLE), United States Government Printing.

Renard, K.G. and Freimund, J.R. 1994. Using monthly precipitation data to estimate the R-factor in the revised USLE. *Journal of Hydrology* 157(1-4): 287-306. https://doi.org/10.1016/0022-1694(94)90110-4

Robinson, A., Lehmann, J., Barriopedro, D., Rahmstorf, S. and Coumou, D. 2021. Increasing heat and rainfall extremes now far outside the historical climate. *npj Climate and Atmospheric Science* 4 (45). https://doi.org/10.1038/s41612-021-00202-w

Santosa, P.B., Mitani, Y. and Ikemi, H. 2010. Estimation of RUSLE EI_{30} based on 10 min interval rainfall data and GIS-based development of rainfall erosivity maps for Hitotsuse basin in Kyushu Japan. In: *18th International Conference on Geoinformatics*, Beijing, China, 2010, pp. 1-6, https://doi.org/10.1109/GEOINFORMATICS.2010.5568195

Santra, P., Goyal, R.K., Tewari, J.C., Roy, M.M. and Singh, J.P. 2014. Assessment of potential soil loss rate by wind and water erosion in Jodhpur region of western Rajasthan, India. In: *Global Soil Map - Basis of the Global Spatial Soil Information System* (Eds. D. Arrouays, N. McKenzie, J. Hempel, A.R. de Forges and A. McBratney), pp. 139-143. CRC Press, Taylor & Francis Group, London, https://doi.org/10.1201/b16500-28

Sartori, M., Philippidis, G., Ferrari, E., Borrelli, P., Lugato, E., Montanarella, L. and Panagos, P. 2019. A linkage between the biophysical and the economic: Assessing the global market impacts of soil erosion. *Land Use Policy* 86: 299-312. https://doi.org/10.1016/j.landusepol.2019.05.014

Schmidt, S., Alewell, C., Panagos, P. and Meusburger, K. 2016. Regionalization of monthly rainfall erosivity patterns in Switzerland. *Hydrology and Earth System Sciences* 20(10): 4359-4373. https://doi.org/10.5194/hess-20-4359-2016

Shamshad, A., Azhari, M.N., Isa, M.H. al, Hussin, W.M.A.W. and Parida, B.P. 2008. Development of an appropriate procedure for estimation of RUSLE EI_{30} index and preparation of erosivity maps for Pulau Penang in Peninsular Malaysia. *Catena* 72(3): 423-432. https://doi.org/10.1016/j.catena.2007.08.002

Singh, J. and Singh, O. 2020. Assessing rainfall erosivity and erosivity density over a western Himalayan catchment, India. *Journal of Earth System Science* 129(1): 97. https://doi.org/10.1007/s12040-020-1362-8

Striffler, W.D., Tejwani, K.G. and Babu, R. 1979. A note on rainfall intensity classes for tropical countries like India. *Indian Journal of Soil Conservation* 7(1): 60-61.

Tu, A., Xie, S., Li, Y., Liu, Z. and Shen, F. 2023. Effect of fixed time interval of rainfall data on calculation of rainfall erosivity in the humid area of south China. *Catena* 220: 106714. https://doi.org/10.1016/j.catena.2022.106714

Verstraeten, G., Poesen, J., Demarée, G. and Salles, C. 2006. Long-term (105 years) variability in rain erosivity as derived from 10 min rainfall depth data for Ukkel (Brussels, Belgium): Implications for assessing soil erosion rates. *Journal of Geophysical Research Atmospheres* 111(D22). https://doi.org/10.1029/2006JD007169

Williams, J.R. and Berndt, H.D. 1972. Sediment yield computed with universal equation. *Journal of Hydraulics Division* 98(12): 2087-2098. https://doi.org/10.1061/JYCEAJ.0003498

Williams, R.G. and Sheridan, J.M. 1991. Effect of rainfall measurement time and depth resolution on EI calculation. *Transactions of the American Society of Agricultural Engineers* 34(2): 402-406. https://doi.org/10.13031/2013.31675

Wischmeier, W.H. and Smith, D.D. 1978. Predicting rainfall erosion losses: A guide to conservation planning. *Agriculture Handbook*, Volume 537, United States Department of Agriculture, Washington DC, USA.

Xie, Y., Yin, S.Q., Liu, B.Y., Nearing, M.A. and Zhao, Y. 2016. Models for estimating daily rainfall erosivity in China. *Journal of Hydrology* 535: 547-558. https://doi.org/10.1016/j.jhydrol.2016.02.020

Yin, S., Xie, Y., Nearing, M.A. and Wang, C. 2007. Estimation of rainfall erosivity using 5- to 60 minute fixed-interval rainfall data from China. *Catena* 70(3): 306-312. https://doi.org/10.1016/j.catena.2006.10.011

Yin, S.-Q., Xie, Y., Liu, B. and Nearing, M.A. 2015. Rainfall erosivity estimation based on rainfall data collected over a range of temporal resolutions. *Hydrology and Earth System Sciences* 19(10): 4113-4126. https://doi.org/10.5194/hess-19-4113-2015

Yu, B. 1998. Rainfall erosivity and its estimation for Australia's tropics. *Australian Journal of Soil Research* 36(1): 143-166. https://doi.org/10.1071/S97025

Yu, B. and Rosewell, C.J. 1996. Rainfall erosivity estimation using daily rainfall amounts for South Australia. *Australian Journal of Soil Research* 34(5): 721-733. https://doi.org/10.1071/SR9960721

Yue, T., Xie, Y., Yin, S., Yu, B., Miao, C. and Wang, W. 2020. Effect of time resolution of rainfall measurements on the erosivity factor in the USLE in China. *International Soil and Water Conservation Research* 8: 373-382. https://doi.org/10.1016/j.iswcr.2020.06.001

Zhang, W., Zhou, J., Feng, G., Weindorf, D.C., Hu, G. and Sheng, J. 2015. Characteristics of water erosion and conservation practice in arid regions of Central Asia: Xinjiang, China as an example. *International Soil and Water Conservation Research* 3(2): 97-111. http://dx.doi.org/10.1016/j.iswcr.2015.06.002

Printed in December 2025